Study of the interaction between light and nanoantennas in Tip-Enhanced Raman Spectroscopy

Hudson Miranda
Graduate Program in Electrical Eng.
Universidade Federal de Minas Gerais
Belo Horizonte, Brazil
hudson@labns.com.br

Cassiano Rabelo
Graduate Program in Electrical Eng.
Universidade Federal de Minas Gerais
Belo Horizonte, Brazil
cassianorabelo@ufmg.br

Thiago L. Vasconcelos
Divisão de Metrologia de Materiais
Inmetro
Rio de Janeiro, Brazil
tlvasconcelos@inmetro.gov.br

Luiz Gustavo Cançado
Departamento de Física
Universidade Federal de Minas Gerais
Belo Horizonte, Brazil
cancado@fisica.ufmg.br

Ado Jorio
Departamento de Física
Universidade Federal de Minas Gerais
Belo Horizonte, Brazil
adojorio@fisica.ufmg.br

***Abstract*—The interaction of light with nanometric metallic structures - nanoantennas - is of particular interest for material analysis techniques such as Tip Enhanced Near-Field Optical Microscopy (TENOM) and, specifically, Tip Enhanced Raman Spectroscopy (TERS). In these scenarios, the nanoantenna's response to an excitation provided by a tightly focused laser beam is essential in order to qualify the system's lateral resolution and signal-to-noise ratio. This work proposes an apparatus that enables the study of the nanoantenna's response in the focal region of light provided by a high numerical aperture optical system. The apparatus is validated by measuring the Raman scattering intensity distribution around the focal region under different conditions, enabling the precise characterization of the electromagnetic field distribution around the focal region, providing informations regarding alignment tolerance, optical signal enhancement and optical system's Point Spread Function (PSF).**

***Index Terms*—Tip Enhanced Raman Spectroscopy, Nanoantenna, Optical Microscopy, Point Spread Function**

I. Introduction

The spatial limit for lateral resolution imposed to optical microscopy systems, consequence of the diffraction limit, greatly reduces the scope of application of optical characterization techniques in the analysis of nanomaterials [1]. This limitation can be overcome by the combination of the optical microscopy system with a Scanning Probe Microscopy (SPM) system, resulting in Tip-Enhanced Near-Field Optical Microscopy (TENOM) [2]. This family of techniques explores localized emission and amplification provided by a metallic nanoantenna positioned at the focal region of a microscopy imaging system, as shown in Fig. 1. In this configuration, the electromagnetic field around the SPM tip generates localized surface plasmon resonance at the tip's interface with the medium [3]. This phenomenon enables the antenna to operate as a nanometric light source, locally exciting the material in its near-field [4]. Additionally, it also enables the tip to amplify the optical signal emitted by the sample as a consequence of the excitation. These two contributions allow the acquisition of optical images with nanometric resolution, usually around 10 nm, while also improving the signal-to-noise ratio [2].

This work has been funded by CNPq grant 153532/2016-5, Embrapii, Codemge, Fapemig, CAPES and Finep.

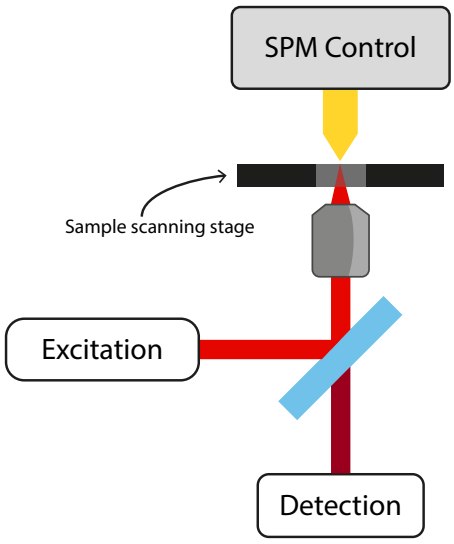

Fig. 1. In a TENOM system, an excitation source, usually a laser beam, is focused onto sample through an objective lens. The same objective then collects the scattered light, guiding it to an optical detector. The SPM control system is responsible for positioning the nanoantenna with nanometric precision with respect to the focal spot area. This positioning is critical in order to obtain spatial resolution beyond the diffraction limit.

TENOM can be used in association with different optical phenomena, such as luminescence, fluorescence and Raman scattering. This work focuses on the last one, which, when combined with TENOM, results on a technique called Tip-

978-1-7281-2109-3/19/$31.00 © 2019 IEEE

Enhanced Raman Spectroscopy (TERS) [5]. Raman spectroscopy is capable of providing information regarding composition, structure and function of materials at a micrometric scale [6], while TERS provides the same categories of information, but at a nanometric scale.

A key aspect for the proper operation of a TERS system is the fine alignment between the nanoantenna and the optical system's focal spot [7]. To better understand the tolerances involved in this alignment, an apparatus for scanning the nanoantenna around the focal region was developed. As it will be shown in this work, the apparatus is able to define limits for the alignment tolerance, the optical system's Point Spread Function (PSF) and nanoantenna's signal enhancement.

II. Scanning Hardware

The experimental setup consists of an inverted confocal microscope setup in conjunction with a home-made atomic force microscope (AFM). The AFM system is composed of an scanning probe microscope (SPM) controller and a scanhead, which is responsible for the nanometric antenna position in a 3D space. The scanhead actuator structure is based on a piezoelectric tube stack, as shown in Fig. 2. With this setup it is possible to keep a constant distance between the nanoantenna and the sample's surface during scanning procedures while also providing XY plane movement for alignment with the laser's focal spot.

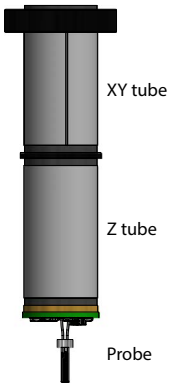

Fig. 2. The probe, containing the nanoantenna, is attached to the end of a piezo tube stack and then housed in a metal cylinder supported by the scanhead. The bottom element in the piezo stack is responsible for movements along the vertical axis (Z). The upper element in the stack is divided into four segments to enable contraction/dilation of different sections of the tube, generating a deflection of the probe along the horizontal plane (XY). The scanhead concept is based on Refs. [8], [9]

In order to perform scanning procedures with the nanoantenna, a mechanism to move the XY tube automatically and a means to read optical signals must be implemented. Fig. 3 displays a system that performs these tasks. A process computer, which controls the procedure, sends digital signals representing XY positions to a DAC (Model: NI9263). The DAC converts the position signal to a low voltage analog signal with a symmetric 2.5V range, which is then sent to a voltage amplifier that converts it to a 95 V symmetric range. The high voltages are then directly applied to the piezo tube faces.

The system also provides two optical sensor interfaces to acquire measurements while scanning. The first is a photon counter that can be tunned to a particular wavelength by associating it with an optical bandpass filter. The counter sends a Transistor-Transistor Logic (TTL) pulse to an Arduino Nano every instant a photon is detected. The Arduino counts the pulses for an adjustable period of time (exposure time) and relays the values to the process computer. The second optical detector, a spectrometer capable of acquiring optical spectra, can be triggered via TTL pulse in order to synchronize acquisitions with the nanoantenna's movement from one pixel to another in the scan region. Additionally, the spectrometer transmits the results directly to the process computer via USB (this communication is handled by the spectrometer's proprietary software).

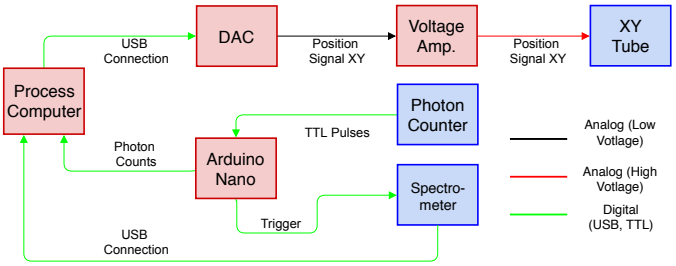

Fig. 3. Diagram showcasing the automated components required to perform raster scanning procedures with a TENOM probe while performing optical signal (spectrum of photon counts) acquisitions for each pixel in the defined scanning area.

III. Control Software

The control software is responsible for interfacing with the DAC and the micro-controller (Arduino Nano) synchronizing the nanoantenna's raster scan with acquisitions performed by the optical sensors. The software also provides a graphical user interface (GUI) that allows moving the probe in the XY plane using the keyboard's arrow keys with an adjustable step size, as shown in Fig. 4. There is also a context window bringing the necessary configuration parameters for scanning and a viewing area to inspect scan results in real time.

IV. Results

A. Point Spread Function Estimation

In order to estimate the optical system's point spread function, the focal region must be scanned with a point-like element. This can be performed with two different approaches: (a) scanning the focal region with a single luminescent molecule deposited in the sample scanning stage [10] or (b) scanning the focal region with the nanoantenna, using the developed scanning apparatus. These two approaches are depicted in Fig. 5.

For the single molecule scan, Nile Blue A molecules (CAS: 3625-57-8) stabilized by a PMMA (CAS: 9011-14-7) thin film were used. The choice for Nile Blue was a consequence

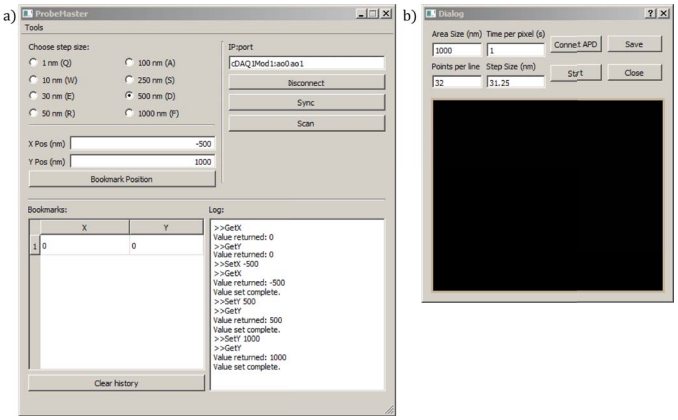

Fig. 4. GUI for the scanning system. The interface consists of a main window (a) that provides functionality for manual probe movement and a context window (b) providing functionality for, scan configuration and visualization. The software was developed in C++ and was based on the Qt Toolkit.

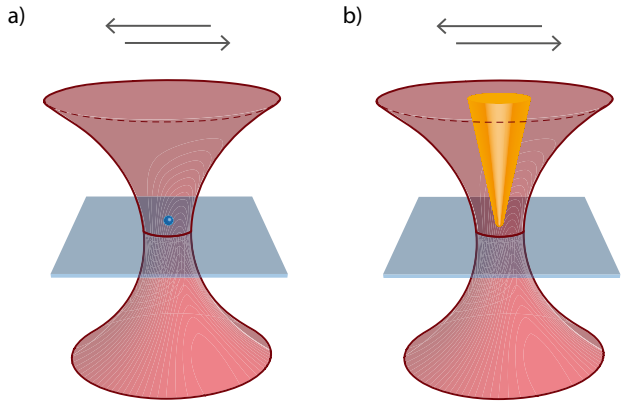

Fig. 5. The focal region can be scanned by emitting sources that are considerably smaller than the focal volume. The figure depicts the scan using (a) a Nile Blue molecule and (b) a TERS probe. In the images, the red hyperboloid represents the focal region and the blue slice represents the focal plane.

of its absorption near 633 nm [11], which is the excitation wavelength for the Helium-Neon laser in the experimental setup. Another benefit of Nile Blue is that its luminescence response is maximum when the dipole defined by the molecule is aligned with the exciting electromagnetic field [4]. Thus, in the experimental configuration, where the field at the focal region is predominantly vertical due to the radial polarization of the excitation laser, only upright molecules provide a symmetric PSF [4]. Our results with the Nile Blue molecules are fully consistent with previous results in the literature [10].

In the case of the probe scan, a graphene sample was exfoliated over a glass substrate in order to obtain a spatially uniform Raman signal generator around the focal region. With the substrate static a Plasmon-Tunned Tip Pyramid (PTTP) TERS probe was used to be scanned over the sample [12]. The results for both scans, using a photon counter as a detector, are shown on Fig. 6.

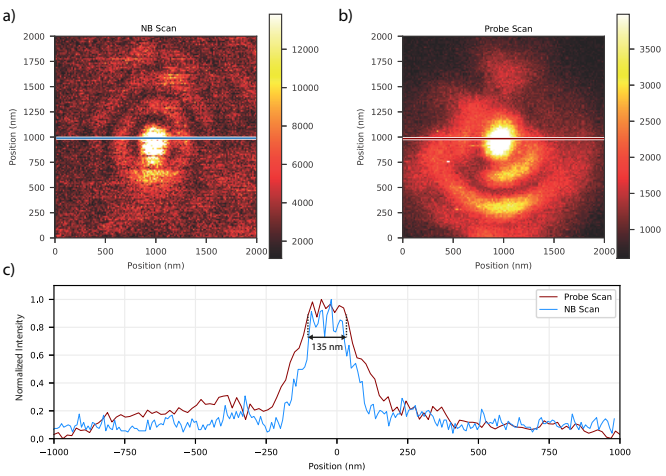

Fig. 6. (a) Luminescence mapping of a single Nile Blue molecule by a photon counter while scanning the sample over the focal spot; (b) Raman map of one of graphene's vibrational mode (2D band [6]) intensity generated by the photon counter while scanning the probe over the sample; (c) Cross section of each map as marked in (a) and (b). The width indicated is for a 90% intensity threshold in the probe scan.

Both scan types yield images of a central hot spot encircled by concentric disks, which is the general shape of an Airy disk. This is the expected shape of the PSF of a properly aligned microscopy setup [4]. The radius of an Airy disk can be defined as the distance between the central maximum and the first local minimum and can be calculated via the Equation:

$$r = 0.61\frac{\lambda}{\mathrm{NA}}, \tag{1}$$

where r is the disk radius, λ is the excitation wavelength and NA is the numerical apperture. For the experimental setup the parameters $\lambda = 632.8\ nm$ and $NA = 1.4$ result in a radius of 276 nm. Nevertheless, as the Nile Blue only responds to the electric field component perpendicular to the sample plane, the scanned image only contains this component of the PSF, which simulations estimate to have a 190 nm radius [4]. The simulated value is in line with the observed radius of 210 nm in Fig. 6(a). In contrast, the probe scan's Airy Disk radius was measured in Fig. 6(b) as 250 nm. This 40 nm difference between the probe scan and the single molecule scan can be attributed to the difference in size of the scanning elements, since the probe's apex diameter is in the range of tens of nanometers, thus not considerable a zero-dimensional structure. This implicates that the probe scan's intensity map could be used for estimating the tip's apex diameter.

Fig. 6(c) shows a cross section of the Nile Blue (blue trace) and TERS probe (red trace) scans along the central line shown in Figs. 6(a) and (b), respectively. The probe scan gives a measure of the local TERS enhancement, providing insight on the alignment tolerance between the probe and the laser in order to obtain a satisfactory enhancement. Considering a region with $> 90\%$ intensity from the maximum, a delimiting radius centered on the hot spot's center with a diamenter of

135 nm can be defined. This region is expected to increase as the nanoantenna's apex becomes broader.

B. Optimal Focal Plane for TENOM

The focal plane of an objective lens is the plane perpendicular to its axis passing through the focal point. For standard optical measurements, this is the optimal distance for imaging in terms of lateral resolution and signal to noise ratio. This doesn't hold for TERS imaging, as the light must interact with the sample and the probe, which is above the sample's plane. To showcase this aspect, an experiment consisting of successive probe scans was performed while varying the objective lens' position and, consequently, the focal plane. The initial position for the experiment was defined from an optimized condition for Raman signal on a graphene sample without the presence of the TERS probe. From this initial condition a scan was performed obtaining the result for Position 0 shown in Fig. 7. In sequence, the focal plane was shifted up in two equal steps of 0.3 ± 0.1 μm (performed by a stepper motor), generating Position 1 and Position 2 images. The focal plane was then brought back to the initial condition and another scan was performed to validate the focal plane's return, as the objective lens positioning system is an open-loop. The focal plane was then shifted downwards using the same step-size, away from the tip, obtaining Position -1 and Position -2 images.

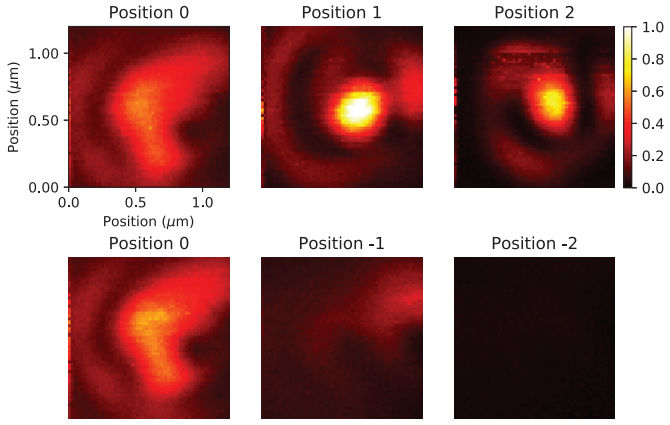

Fig. 7. Successive probe scans performed on graphene's 2D band while varying the objective lens' position (focus) between Positions 0, 1, 2, -1 and -2. Position 0 was obtained by optimizing the Raman signal on a graphene sample without the tip. Positions 1 and -1 are equidistant from Position 0, but the first is located focusing above the sample plane and the second below the sample plane. The same applies for Positions 2 and -2.

Fig. 7 shows that Position 1 presents the optimal focal condition for TERS, as it contains the most intense hot spot. Position 2 indicates that this signal increasing trend is not monotonic, as the hot spot loses amplitude. These higher enhancements, compared to Position 0, can be attribute to an increase of the vertical component of the incident electric field at the probe's body as the focal plane is shifted up. Furthermore, as the focal plane is shifted below the sample plane, the overall signal intensity falls drastically. This observation is consistent with the fact that the focal spot is more distant from the probe and the sample in this scenario.

The scans contained in Fig. 7 are able to provide a measure of the probe's signal enhancement also considering focus refinement. Formally the TERS enhancement is calculated by computing the ratio between a Raman band peak amplitude in the presence of a tip divided by the amplitude of the same band without the present of the tip. For this experiment, however, solely the photon counts in the Raman 2D band's region (mixed with background not related to Raman scattering) were measured. An approximation of the enhancement can be obtained by calculating the ratio between the brightest and dimmest pixels in the probe scan images. Table I lists the values for all the focus positions.

TABLE I
INTENSITY RATIO

	Min	**Max**	**Ratio**
Pos 0	3,610	19,220	5.32
Pos 1	2,800	33,810	12.01
Pos 2	1,380	24,500	17.75
Pos -1	2,420	10,250	4.24
Pos -2	1,300	2,330	1.79

*Min and Max are in photon counts

Table I shows that Positions 1 and 2 are the most favorable positions for TERS measurements, but with Position 2 presenting the largest enhancement. Such phenomenon occurred due to a significant reduction in the background for this focal position, compared to Position 1. This showcases the importance of analyzing the actual Raman spectra, where the background noise contribution can be eliminated, during alignment procedures prior to performing TERS measurements.

V. CONCLUSION

The capability of scanning a TENOM probe over a nanometric area allows for a deeper understanding of the focal region. Two key findings with practical implications for TENOM experiments can be derived from the results: the lateral alignment tolerance of approximately 135 nm for a $> 90\%$ efficiency and the proper positioning of the focal plane a few hundreds of nanometers towards the probe to increase signal intensity. These parameters are critical for the design of an alignment system for TENOM. The probe scans are also useful to provide two main figures of merit for TERS probes: the probe apex diameter (as estimated by the PSF image) and the nanoantenna's enhancement factor.

Probe scanning systems similar to the one presented on this work are present in commercial TENOM systems with automatic probe alignment, such as NT-MDT's NTEGRA SPECTRA II. Nevertheless, these systems are not used for studying the probe's optical response in depth.

ACKNOWLEDGMENT

The authors acknowledge fruitful discussions and significant contributions by Professors Achim Hartschuh and Lukas Novotny.

REFERENCES

[1] L. Novotny and S. J. Stranick, "Near-Field Optical Microscopy and Spectroscopy With Pointed Probes," *Annual Review of Physical Chemistry*, vol. 57, no. 1, pp. 303–331, 2005.

[2] A. Hartschuh, "Tip-Enhanced Near-Field Optical Microscopy," *Angewandte Chemie International Edition*, vol. 47, no. 43, pp. 8178–8191, oct 2008. [Online]. Available: http://doi.wiley.com/10.1002/anie.200801605

[3] T. L. Vasconcelos, B. S. Archanjo, B. Fragneaud, B. S. Oliveira, J. Riikonen, C. Li, D. S. Ribeiro, C. Rabelo, W. N. Rodrigues, A. Jorio, C. A. Achete, and L. G. Cançado, "Tuning Localized Surface Plasmon Resonance in Scanning Near-Field Optical Microscopy Probes," *ACS Nano*, vol. 9, no. 6, pp. 6297–6304, 2015.

[4] L. Novotny and B. Hecht, *Principles of Nano-Optics*. Cambridge: Cambridge University Press, 2012. [Online]. Available: http://ebooks.cambridge.org/ref/id/CBO9780511794193

[5] R. M. Stöckle, Y. D. Suh, V. Deckert, and R. Zenobi, "Nanoscale chemical analysis by tip-enhanced Raman spectroscopy," *Chemical Physics Letters*, vol. 318, no. 1-3, pp. 131–136, 2000. [Online]. Available: http://linkinghub.elsevier.com/retrieve/pii/S0009261499014517

[6] A. Jorio, R. Saito, G. Dresselhaus, and M. S. Dresselhaus, *Raman Spectroscopy in Graphene Related Systems*. Weinheim: WILEY-VCHVerlag GmbH & Co. KGaA, 2011.

[7] N. Kumar, B. M. Weckhuysen, A. J. Wain, and A. J. Pollard, "Nanoscale chemical imaging using tip-enhanced Raman spectroscopy," *Nature Protocols*, vol. 14, no. 4, pp. 1169–1193, apr 2019. [Online]. Available: http://www.nature.com/articles/s41596-019-0132-z

[8] A. Hartschuh, E. J. Sánchez, X. S. Xie, and L. Novotny, "High-Resolution Near-Field Raman Microscopy of Single-Walled Carbon Nanotubes," *Physical Review Letters*, vol. 90, no. 9, p. 095503, mar 2003. [Online]. Available: https://link.aps.org/doi/10.1103/PhysRevLett.90.095503

[9] K. Karrai and R. D. Grober, "Piezoelectric tip-sample distance control for near field optical microscopes," *Applied Physics Letters*, vol. 66, no. 14, pp. 1842–1844, 2002.

[10] P. Anger, P. Bharadwaj, and L. Novotny, "Enhancement and Quenching of Single-Molecule Fluorescence," *Physical Review Letters*, vol. 96, no. 11, p. 113002, mar 2006. [Online]. Available: https://link.aps.org/doi/10.1103/PhysRevLett.96.113002

[11] H. Du, R.-c. A. Fuh, J. Li, L. A. Corkan, and J. S. Lindsey, "PhotochemCAD: A Computer-Aided Design and Research Tool in Photochemistry," *Photochemistry and Photobiology*, vol. 68, no. 2, pp. 141–142, aug 1998. [Online]. Available: https://omlc.org/spectra/PhotochemCAD/html/005.html

[12] T. L. Vasconcelos, B. S. Archanjo, B. S. Oliveira, R. Valaski, R. C. Cordeiro, H. G. Medeiros, C. Rabelo, A. Ribeiro, P. Ercius, C. A. Achete, A. Jorio, and L. G. Cançado, "Plasmon-Tunable Tip Pyramids: Monopole Nanoantennas for Near-Field Scanning Optical Microscopy," *Advanced Optical Materials*, vol. 6, no. 20, p. 1800528, oct 2018. [Online]. Available: http://doi.wiley.com/10.1002/adom.201800528